Robust Kalman filter for Tuberculosis Incidence Time Series Forecasting ⋆

Andres L. Jutinico * **Erika Vergara** *
Carlos Enrique Awad García ** **Maria Angélica Palencia** **
Alvaro David Orjuela-Cañon ***

* *Mechanical, Electronics and Biomedical Engineering Faculty, Universidad Antonio Nariño, Bogota D.C., Colombia (e-mail: ajutinico@uan.edu.co, paoli1982@gmail.com).*
** *Subred Integrada de Servicios de Salud Centro Oriente, Bogota D.C., Colombia (e-mail: carlosawad@gmail.com, angeliquitapalencia@gmail.com)*
*** *School of Medicine and Health Sciences, Universidad del Rosario, Bogota D.C., Colombia (e-mail: alvaro.orjuela@urosario.edu.co)*

Abstract: Governments must detect and treat people with tuberculosis, also prevent the uninfected community. In this sense, must promote the study of algorithms for the prediction of the epidemic trend. This paper addresses the forecasting of tuberculosis cases in Bogota, considering health surveillance system data from 2007-2020. Forecasts are obtained using the Kalman Filter and the Robust Kalman Filter. Results show better performance using the robust filter for six-week tuberculosis cases prediction.

Keywords: Tuberculosis, Time Series, Forecasting, Kalman filter, Auto-Regressive models.

1. INTRODUCTION

Tuberculosis (TB) is an infectious disease and one of the top 10 causes of death worldwide. In 2019, about 10 million people developed TB, and 1.4 million died (World Health Organization, 2020). In Colombia, during 2020, 11,390 people became ill with TB, of which 10,632 were new cases, revealing that in the country, the incidence rate of tuberculosis is 20.88 per 100,000 inhabitants (Ospina-Martinez et al., 2021). This disease is caused by Mycobacterium tuberculosis, and its more known form affects the lungs (pulmonary TB), being contracted by airways when people infected with TB cough and expelled the bacteria.

The prediction of the epidemic trend from surveillance data can be used for the health system to prevent and control the occurrence of TB cases. In state-of-the-art, there are several forecasting methods for infectious diseases (Zheng et al., 2021). However, TB forecasting is still a challenge given the abrupt changes of trend and dispersion of TB incidence relative to each region or country. Notice that the behavior of this epidemic depends on several factors related to the contagious disease, government laws, and socioeconomic factors. Some of these factors are random and variables in time, e.g., the increase of immigrant populations, representing a significant portion of TB epidemics (Kavanagh et al., 2020). This paper addressed the prediction of TB cases using the Robust Kalman Filter (RKF) and Auto-Regressive (AR) models.

Zheng et al. (2021) performed the time series analysis under the hybrid method Box-Jenkins and Elman neural network to predict TB incidence in Kashgar (China), where there is a high rate of TB occurrence. They conclude that this AR hybrid method is effective and can predict TB incidence in this place. Ku and Dodd (2019) developed a prediction model regarding the impact of Taiwan population aging on the incidence of tuberculosis. The model developed indicates that by 2035 the TB incidence rate will decrease by 54 % compared to 2015. Nonetheless, they emphasize that they will have higher TB mortality rates for older adults. Liu et al. (2019) addressed the pulmonary TB case prediction in southeast China in Jiangsu province, where TB incidence rates are high. They used the Auto-Regressive Integrated Moving Average Model (ARIMA) and the Back-propagation Neural Network (BPNN). Both methods were evaluated to predict seasonality and trend using error indices, where BPNN presented better results for the prediction. Similar results were achieved using a hybrid system incorporating the ARIMA and Nonlinear Auto-Regressive Neural Networks (NAR) (Wang et al., 2017). In (Azeez et al., 2016), the authors compared two methods to forecasting TB incidence and analyzed its seasonality in South Africa. These methods are the Seasonal Auto-Regressive Integrated Moving Average (SARIMA) and Neural Network Auto-Regressive (SARIMA-NNAR).

In Colombia, studies related to time series forecasting are mainly addressed to other types of diseases. The forecasting of Dengue disease was studied in (Martinez-Bello et al., 2017), applying Bayesian hierarchical dynamic generalized linear models and dealt with weekly incidence cases from 2008 to 2015. In (Chowell et al., 2016) have been treated the forecast for Zika disease in the Antioquia region using the generalized Richards model. In (ArunKumar et al.,

⋆ This work is supported by the Ministerio de Ciencia y Tecnología – Minciencias from Colombia under grant 123380762899.

2021) performed a study to forecast the epidemiological trends of the COVID-19 pandemic for 16 countries, including Colombia; for this, the authors used the ARIMA and SARIMA models. We highlight that there are not enough studies about time series forecasting related to TB in Colombia. The methods used in this article to forecast the TB cases in Bogota consider AR models from training data. We compared the performance of the prediction using the Kalman Filter with different order of nominal models. We also regard the uncertainties of the trained models and use the RKF to obtain the forecast. Finally, the accuracy of prediction is evaluated.

The rest of this paper is organized as follows: Section 2 introduce the Auto-Regressive model for data prediction; Section 3 introduce the Kalman filter; in Section 4 is presenting the Robust Kalman filter; in Section 5 are explained the results and in Section 6 the conclusions.

2. AUTO-REGRESSIVE MODEL FOR DATA PREDICTION

In this paper, we use the number of reported cases of pulmonary TB in Bogota city from 2007 to 2020 extracted from the Health National Institute (INS in Spanish). The time series is formed by confirmed cases week by week, reported by the SIVIGILA (Colombian Vigilance in Public Health System, by its acronym in Spanish). Figure 1 shows the confirmed cases of pulmonary TB in Bogota during 2007-2020. The time series is divided into two data groups for identification and validation of a state-space model. We use the Numerical algorithms for Subspace State Space System Identification (N4SID) technique to obtain this model (Van Overschee and De Moor, 1994). The model in (1)-(2) is describing in a canonical way, which allows forecasting states according to the order of the system. In this model $x_k \in \mathbb{R}^n$ is the state vector to be estimated with its corresponding state variables (χ), $y_k \in \mathbb{R}^p$ is the measurement signal, $\omega_k \in \mathbb{R}^{m_2}$ is the state noise and $v_k \in \mathbb{R}^t$ is the output noise. The nominal matrices F, G and C have appropriated dimensions.

$$\begin{bmatrix} \chi_{k+1} \\ \chi_{k+2} \\ \vdots \\ \chi_{k+n-1} \\ \chi_{k+n} \end{bmatrix} = \underbrace{\begin{bmatrix} 0 & 1 & 0 & \cdots & 0 \\ 0 & 0 & 1 & \cdots & 0 \\ \vdots & \vdots & \vdots & \ddots & \vdots \\ 0 & 0 & 0 & \cdots & 1 \\ f_0 & f_1 & f_2 & \cdots & f_{n-1} \end{bmatrix}}_{F} \begin{bmatrix} \chi_k \\ \chi_{k+1} \\ \chi_{k+2} \\ \vdots \\ \chi_{k+n-1} \end{bmatrix} + \underbrace{\begin{bmatrix} g_{n-1} \\ g_{n-2} \\ g_{n-3} \\ \vdots \\ g_0 \end{bmatrix}}_{G} \omega_k \tag{1}$$

$$y_k = \underbrace{[1\ 0\ 0\ \cdots\ 0]}_{C} \underbrace{\begin{bmatrix} \chi_k \\ \chi_{k+1} \\ \chi_{k+2} \\ \vdots \\ \chi_{k+n-1} \end{bmatrix}}_{x_k} + v_k. \tag{2}$$

3. THE KALMAN FILTER

The Kalman filter aims to find the optimal states estimates $\hat{x}_k^*$, $\hat{x}_{k+1}^*$ by minimize the quadratic criterion (3) subject to model (1)-(2).

$$\underset{\hat{\omega}_k, \hat{v}_k, \hat{x}_k, \hat{x}_{k+1}}{min} \left\{ \| \hat{x}_k - \hat{x}_{k|k-1} \|^2_{P^{-1}_{k|k-1}} + \begin{bmatrix} \hat{\omega}_k \\ \hat{v}_k \end{bmatrix}^T \begin{bmatrix} Q & 0 \\ 0 & R \end{bmatrix}^{-1} \begin{bmatrix} \hat{\omega}_k \\ \hat{v}_k \end{bmatrix} \right\}. \tag{3}$$

The matrices $P_{k|k} \succ 0$, $Q \succ 0$ and $R \succ 0$ are the posteriori estimate covariance, the covariance of the process noise and the covariance of the observation noise, respectively. The update of the matrix $P_{k|k}$ is given by the Riccati equation (4)-(5), and the Kalman gain L_k is given by (6).

$$P_{k|k} = P_{k|k-1} - P_{k|k-1}C^T(R + CP_{k|k-1}C^T)^{-1}CP_{k|k-1}, \tag{4}$$

$$P_{k+1|k} = Q + FP_{k|k}F^T, \tag{5}$$

$$L_k = P_{k|k-1}C^T(R + CP_{k|k-1}C^T)^{-1}. \tag{6}$$

Therefore, the current states of the model (1) are estimated by the Kalman filter as follows,

$$\hat{x}_{k|k} = \hat{x}_{k|k-1} + L_k(y_k - C\hat{x}_{k|k-1}). \tag{7}$$

The readers can find more details about the Kalman filter in (Sayed, 2008) and (Grewal and Andrews, 2014).

4. THE ROBUST KALMAN FILTER

The Robust Kalman Filter was introduced by Ishihara et al. (2015). Consider the model in (8)-(9) which is a representation of the model (1)-(2), but considering uncertainties in the model,

$$x_{k+1} = (F_k + \delta F_k)x_k + G_k w_k, \tag{8}$$

$$y_k = (C_k + \delta C_k)x_k + v_k, \qquad k \geq 0. \tag{9}$$

The uncertain matrices $\delta F_k \in \mathbb{R}^{n\times n}$ and $\delta C_k \in \mathbb{R}^{p\times n}$ are defined as follows,

$$\delta F_k = M_k \Delta_k E_{F_k}, \quad \delta C_k = N_k \Delta_k E_{C_k}, \quad \| \Delta_k \| \leq 1, \tag{10}$$

where, E_{F_k} and E_{C_k} have appropriate dimensions, M_k and N_k are a non zero matrices, and Δ_k is an arbitrary contraction. Assume that x_0, w_k and v_k are mutually independent zero-mean Gaussian random variables with variances $\mathbb{E}\{x_0 x_0^T\} = \Pi_0 \succ 0$, $\mathbb{E}\{w_0 w_0^T\} = Q_k \succ 0$ and $\mathbb{E}\{v_0 v_0^T\} = R_k \succ 0$, respectively. The RKF is deduced based on the solution of the optimization problem (11)-(12). The aim is to obtain a robust filtering that minimizes the influence of the state noise ω_k and measurement noise v_k in the states estimate of the model (8)-(9), with $e_k = \hat{x}_k - \hat{x}_{k|k-1}$.

$$\min_{\hat{\omega}_k, \hat{v}_k, \hat{x}_k, \hat{x}_{k+1}} \max_{\delta F_k, \delta C_k} \{\mathcal{J}_k\}, \tag{11}$$

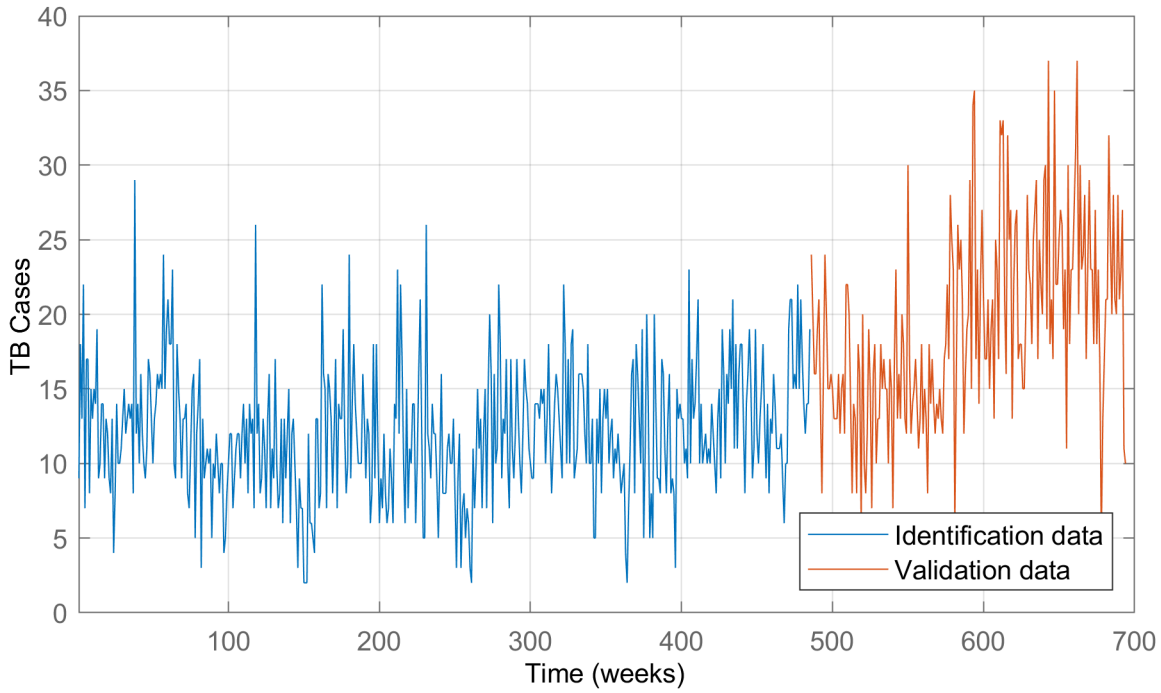

Fig. 1. Reported TB cases in Bogota for 2007-2020 period.

$$\mathcal{J}_k := \begin{bmatrix} e_k \\ \hat{\omega}_k \\ \hat{v}_k \\ \hat{x}_k \\ \hat{x}_{k+1} \end{bmatrix}^T \begin{bmatrix} P_{k|k-1}^{-1} & 0 & 0 & 0 & 0 \\ 0 & Q_k^{-1} & 0 & 0 & 0 \\ 0 & 0 & R_k^{-1} & 0 & 0 \\ 0 & 0 & 0 & 0 & 0 \\ 0 & 0 & 0 & 0 & 0 \end{bmatrix} \begin{bmatrix} e_k \\ \hat{\omega}_k \\ \hat{v}_k \\ \hat{x}_k \\ \hat{x}_{k+1} \end{bmatrix} +$$

$$\left\{ \begin{bmatrix} -I & 0 & 0 & I & 0 \\ 0 & G_k & 0 & F_k + \delta F_k & -I \\ 0 & 0 & I & C_k + \delta C_k & 0 \end{bmatrix} \begin{bmatrix} e_k \\ \hat{\omega}_k \\ \hat{v}_k \\ \hat{x}_k \\ \hat{x}_{k+1} \end{bmatrix} - \begin{bmatrix} x_{k|k-1} \\ 0 \\ y_k \end{bmatrix} \right\}^T \mu\{\bullet\}. \tag{12}$$

The framework to describe the RKF in the filtered form can be seen in Table 1 and their auxiliary matrices in (13)-(16). To ensure the optimal response, the parameter $\alpha \geq 1$ is selected.

$$\hat{\lambda}_k = (1+\alpha) \left\| \begin{matrix} \mu M_k^T M_k & 0 \\ 0 & \mu N_k^T N_k \end{matrix} \right\|, \tag{13}$$

$$\mathcal{W}_{1,k} = \begin{bmatrix} (\mu^{-1} I - \hat{\lambda}_k^{-1} M_k M_k^T) & 0 \\ 0 & \hat{\lambda}_k^{-1} I \end{bmatrix}, \tag{14}$$

$$\mathcal{W}_{2,k} = \begin{bmatrix} (\mu^{-1} I - \hat{\lambda}_k^{-1} N_k N_k^T) & 0 \\ 0 & \hat{\lambda}_k^{-1} I \end{bmatrix}, \tag{15}$$

$$\begin{aligned} \hat{I} &= \begin{bmatrix} I \\ 0 \end{bmatrix}, \hat{F}_k = \begin{bmatrix} F_k \\ E_{F_k} \end{bmatrix}, \hat{G}_k = \begin{bmatrix} G_k \\ 0 \end{bmatrix}, \\ \mathcal{Y}_k &= \begin{bmatrix} y_k \\ 0 \end{bmatrix}, \hat{C}_k = \begin{bmatrix} C_k \\ E_{C_k} \end{bmatrix}, \hat{D}_k = \begin{bmatrix} I \\ 0 \end{bmatrix}. \end{aligned} \tag{16}$$

Table 1. Recursive Robust Kalman Filter.

Consider equation (8), with $\Pi_0 \succ 0$, $Q_k \succ 0$, and $R_k \succ 0$.
Initial Conditions: $P_{0|-1} = \Pi_0$ and $\hat{x}_{0|-1} = 0$.
Step $k \geq 0$**:** Update $\{\hat{x}_{k+1|k}; P_{k+1|k}\}$ and $\{\hat{x}_{k|k}; P_{k|k}\}$.

$$\begin{bmatrix} \hat{x}_{k|k} & \hat{x}_{k+1|k} \\ P_{k|k} & * \\ * & P_{k+1|k} \end{bmatrix}^T = \begin{bmatrix} 0 \\ 0 \\ 0 \\ I \end{bmatrix}^T \begin{bmatrix} \mathfrak{P}_k & 0 & I & 0 \\ 0 & \mathfrak{S}_k & \mathfrak{A}_k & \mathfrak{B}_k \\ I & \mathfrak{A}_k^T & 0 & 0 \\ 0 & \mathfrak{B}_k^T & 0 & 0 \end{bmatrix}^{-1} \begin{bmatrix} 0 & 0 \\ \mathfrak{Z}_k & 0 \\ 0 & 0 \\ 0 & -I \end{bmatrix},$$

$$\mathfrak{P}_k = \begin{bmatrix} P_{k|k-1} & 0 & 0 \\ 0 & Q_k & 0 \\ 0 & 0 & R_k \end{bmatrix}, \mathfrak{S}_k = \begin{bmatrix} \mu^{-1} I & 0 & 0 \\ 0 & \mathcal{W}_{1,k} & 0 \\ 0 & 0 & \mathcal{W}_{2,k} \end{bmatrix},$$

$$\mathfrak{A}_k = \begin{bmatrix} I & 0 & 0 \\ 0 & \hat{G}_k & 0 \\ 0 & 0 & \hat{D}_k \end{bmatrix}, \mathfrak{B}_k = \begin{bmatrix} -I & 0 \\ \hat{F}_k & -\hat{I} \\ \hat{C}_k & 0 \end{bmatrix}, \mathfrak{Z}_k = \begin{bmatrix} -\hat{x}_{k|k-1} \\ 0 \\ \mathcal{Y}_k \end{bmatrix}.$$

5. RESULTS

Accuracy of prediction was evaluated with the Mean Absolute Error (MAE) measure, Mean Absolute Percentage Error (MAPE) and Root Mean Square Error (RMSE), which are commonly employed to assess forecasting models

(Shcherbakov et al., 2013). These performance indices are computed according to:

$$MAE = \frac{1}{\mathcal{N}} \sum_{k=1}^{\mathcal{N}} \mid e_k \mid, \tag{17}$$

$$MAPE = \frac{1}{\mathcal{N}} \sum_{k=1}^{\mathcal{N}} \left| \frac{e_k}{y_k} \right| 100\%, \tag{18}$$

$$RMSE = \sqrt{\frac{1}{\mathcal{N}} \sum_{k=1}^{\mathcal{N}} e_k^2}, \tag{19}$$

where $e_k = y_k - \hat{y}_k$ is the error between the original and the forecasted series, and $\mathcal{N}$ is the number of the values or points in the sequence.

To determine the order of model that allows ten weeks prediction of TB cases, we perform different training with the 70% of time series data, as shown in Fig. 1 in blue color. In this sense, models with different order n were obtained by N4SID algorithm and were made the data estimation using the Kalman filter. From ten-step prediction forward, we calculated the performance indices (17)-(19) and define system order $n = 17$, since this is the case with better behavior, as shown in Fig. 2. Notice that the errors increase for higher values of n. We assume unknown disturbances concerning imperfections from the identification process, considering a standard deviation of 4 TB cases. The filter design was made with covariances $Q = 16$ and $R = 0.1$. The RKF uses the same nominal model and covariances that the Kalman filter. Additionally, the uncertain matrices are defined with the parameters shows in Table 2. The auxiliary parameters are $\alpha = 2$ and $\mu = 1 \cdot 10^5$.

Table 2. Robust Kalman filter parameters.

$E_{F_k} = \begin{bmatrix} f_0 & f_1 & f_2 & \cdots & f_{n-1} \end{bmatrix} \cdot 10^{-3}, \quad E_{C_k} = C \cdot 10^{-3},$
$M_k = \begin{bmatrix} 1 & 1 & \cdots & 1 & 1000 \end{bmatrix}^T \cdot 10^{-3}, \quad N_k = 0.5,$

Table 3 shows training results for ten week TB cases prediction in Bogota. The identification data serie has the number of confirmed case of pulmonary TB during 485 weeks. Notice that the RKF achieve a better performance that the nominal Kalman filter (KF). However, the indice MAPE is higher than 25% for both approaches.

Table 3. Results of the training for ten-week TB cases prediction.

	RMSE	*MAE*	*MAPE*
KF	4.42	3.45	36.33
RKF	3.51	2.72	26.97

The validation data have the information of 209 weeks. Fig. 3 shows the measured signal in brown color and the forecasting TB cases given by the KF and RKF in blue and black colors, respectively. Notice that the KF and RKF allowed forecasting the details from the original series related to the trend. The above is according to RMSE and MAE indices show in Table 4, notice that the approach using the RKF gets lower errors. However, looking at Fig. 3 is evident that prediction does no achieve to hit when the signal has abrupt changes and signal dispersion is higher. Notice that the MAPE index is more suitable to rate this phenomenon.

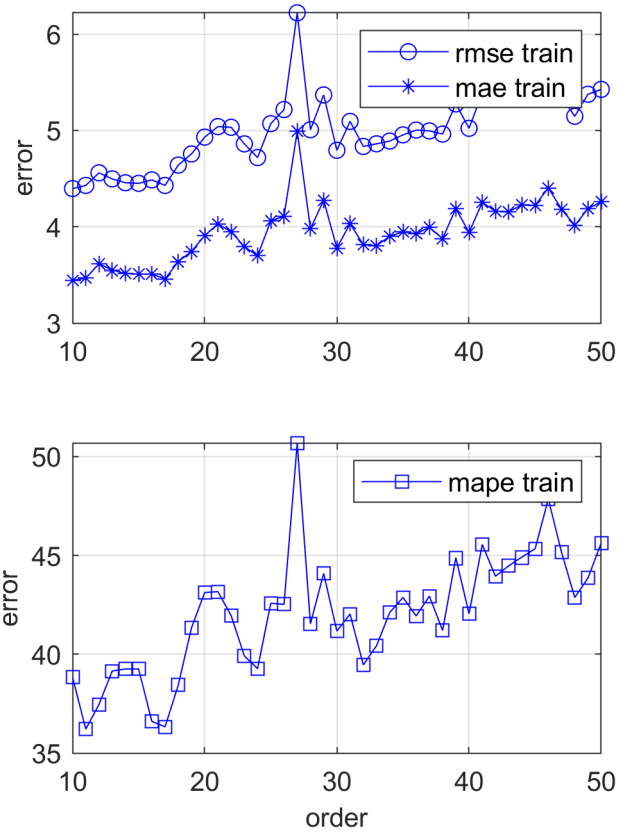

Fig. 2. Selection of the order of model using the Kalman filter and N4SID algorithm. The selected order of model is $n = 17$.

Table 4. Results of the test for ten-week TB cases prediction.

	RMSE	*MAE*	*MAPE*
KF	5.95	4.66	27.40
RKF	4.87	3.85	21.54

Fig. 4 shows the result of diminishing the number of predictions to six weeks for TB cases. In this figure, the measured signal is brown, and the KF and RKF forecast TB cases in blue and black colors, respectively. Notice that getting better results for the RKF. Therefore, TB case forecasting is nearer to actual cases. The above is confirmed by the reduction of error indices in Table 5.

Table 5. Results of the test for six-week TB cases prediction.

	RMSE	*MAE*	*MAPE*
KF	6.44	5.02	29.97
RKF	4.10	3.18	18.01

6. CONCLUSION

In this article, we made weekly forecasting of TB cases in Bogota. A comparative study between the nominal and ro-

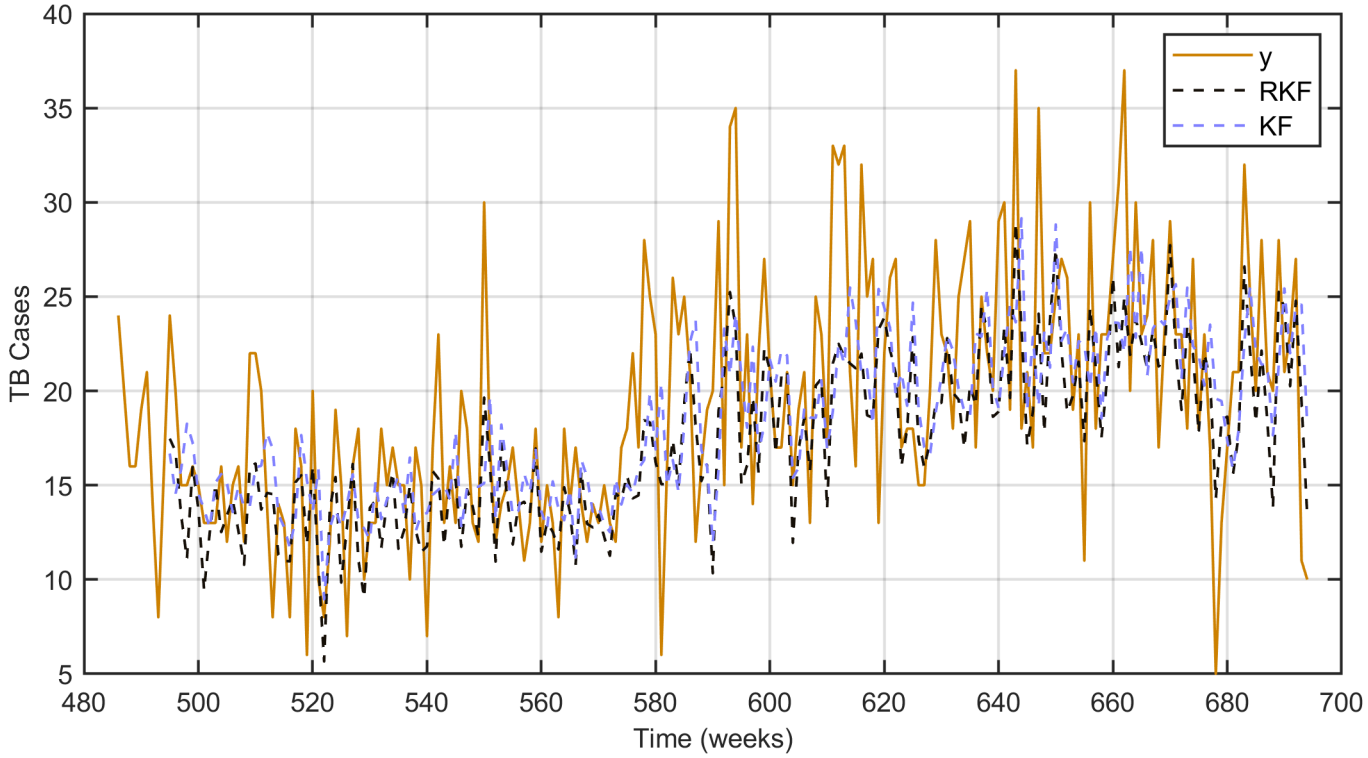

Fig. 3. Results of the test for ten-week TB cases prediction .

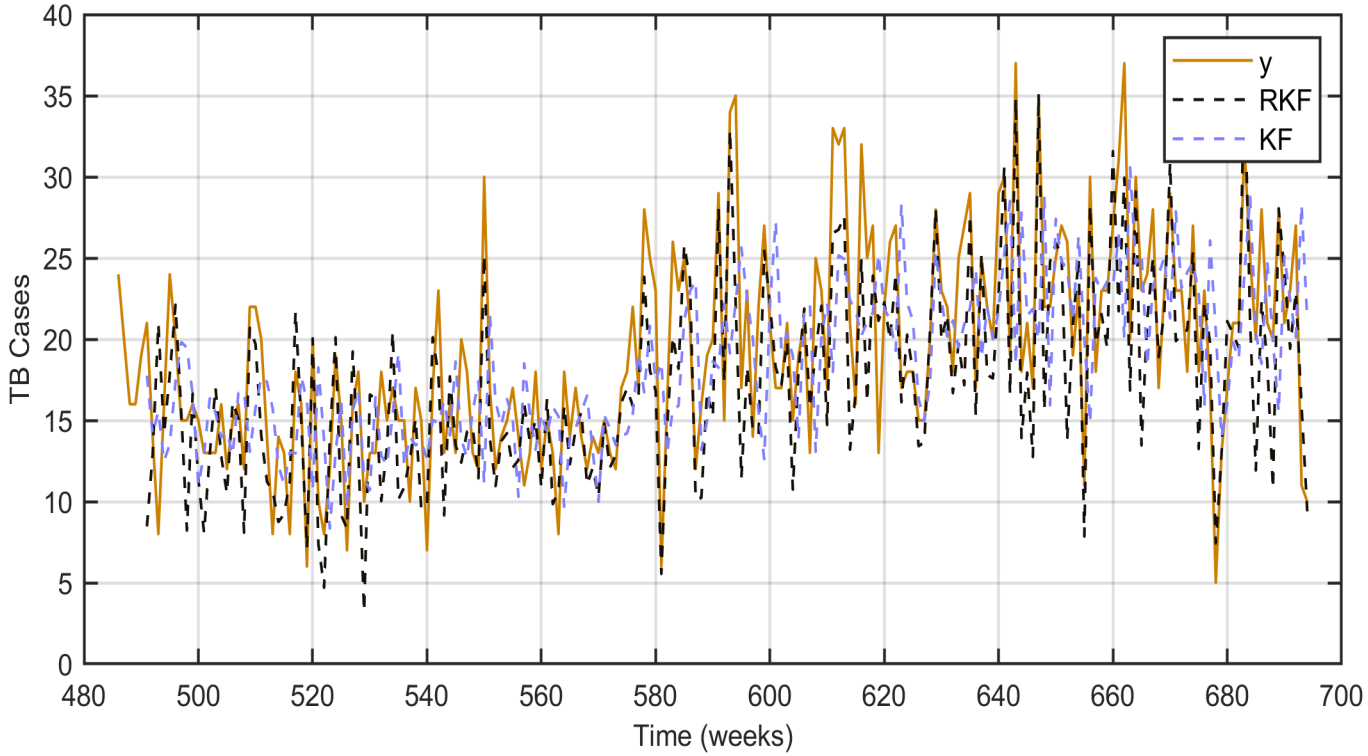

Fig. 4. Results of the test for six-week TB cases prediction .

bust Kalman filter was carried on. The RKF outperformed the KF for the accuracy of prediction. Although the RKF showed low errors to six-week TB cases prediction, we think that other methods must be studied to fit the incidence of TB considering more extended periods forward. For future works, we intend to extend this study using the RKF for discrete-time Markovian jump linear systems (Escalante et al., 2021), also the Extended Kalman filter, the Unscented Kalman Filter, Particle filtering, and deep learning networks.

ACKNOWLEDGEMENTS

Authors acknowledge the support of the Ministerio de Ciencia y Tecnología – Minciencias from Colombia, through founded project 123380762899. In addition, institutions as Universidad Antonio Nariño, the Subred Integrada de Servicios de Salud Centro Oriente and Universidad del Rosario were relevant for the development of this work.

REFERENCES

ArunKumar, K., Kalaga, D.V., Sai Kumar, C.M., Chilkoor, G., Kawaji, M., and Brenza, T.M. (2021). Forecasting the dynamics of cumulative covid-19 cases (confirmed, recovered and deaths) for top-16 countries using statistical machine learning models: Auto-regressive integrated moving average (ARIMA) and seasonal auto-regressive integrated moving average (SARIMA). *Applied Soft Computing*, 103, 107–161.

Azeez, A., Obaromi, D., Odeyemi, A., Ndege, J., and Muntabayi, R. (2016). Seasonality and trend forecasting of tuberculosis prevalence data in eastern cape, south africa, using a hybrid model. *International journal of environmental research and public health*, 13(8), 1–13.

Chowell, G., Hincapie-Palacio, D., Ospina, J., Pell, B., Tariq, A., Daha, S., Moghadas, S., Smirnova, A., Simonsen, L., and Viboud, C. (2016). Using phenomenological models to characterize transmissibility and forecast patterns and final burden of zika epidemics. *PLoS Curr*, 8, 1–21.

Escalante, F.M., Jutinico, A.L., Jaimes, J.C., Terra, M.H., and Siqueira, A.A.G. (2021). Markovian robust filtering and control applied to rehabilitation robotics. *IEEE/ASME Transactions on Mechatronics*, 26(1), 491–502.

Grewal, M.S. and Andrews, A.P. (2014). *Kalman Filtering: Theory and Practice Using Matlab*. John Wiley & Sons, Inc.

Ishihara, J.Y., Terra, M.H., and Cerri, J.P. (2015). Optimal robust filtering for systems subject to uncertainties. *Automatica*, 52, 111 – 117.

Kavanagh, M., Gostin, L.O., and Stephens, J. (2020). Tuberculosis, human rights, and law reform: Addressing the lack of progress in the global tuberculosis response. *PLoS Medicine*, 17(10), 1–9.

Ku, C.C. and Dodd, P. (2019). The PLOS ONE staff (2019) correction: Forecasting the impact of population ageing on tuberculosis incidence. *PLoS ONE*, 14(10), 1–13.

Liu, Q., Li, Z., J, Y., Martinez, L., Zi, U., Javaid, A., Lu, W., and Wang, J. (2019). Forecasting the seasonality and trend of pulmonary tuberculosis in jiangsu province of china using advanced statistical time-series analyses. *Infection and Drug Resistance*, 12, 2311–2322.

Martinez-Bello, D., Lopez-Quilez, A., and Torres-Prieto, A. (2017). Bayesian dynamic modeling of time series of dengue disease case counts. *PLoS Negl Trop Dis*, 11(7), 1–19.

Ospina-Martinez, M.L., Prieto-Alvarado, F.E., Walteros, D., and Quijada-Bonilla, H. (2021). *Comportamiento de la Vigilancia de Tuberculosis, Colombia, 2020*. Instituto Nacional de Salud.

Sayed, A.H. (2008). *Adaptive Filters*. John Wiley & Sons, Inc.

Shcherbakov, M., Brebels, A., Shcherbakova, N., Tyukov, A., Janovsky, T., and Kamaev, V. (2013). A survey of forecast error measures. *World Applied Sciences Journal*, 24, 171–176.

Van Overschee, P. and De Moor, B. (1994). N4SID: Subspace algorithms for the identification of combined deterministic-stochastic systems. *Automatica*, 30(1), 75–93. Special issue on statistical signal processing and control.

Wang, K., Deng, C., Li, J., Zhang, Y., L, X., and Wu, M. (2017). Hybrid methodology for tuberculosis incidence time-series forecasting based on ARIMA and a NAR neural network. *Epidemiol Infect*, 145(6), 118–1129.

World Health Organization (2020). *Global tuberculosis report 2020*. Geneva: World Health Organization.

Zheng, Y., Zhang, X., Wang, X., Wang, K., and Cui, Y. (2021). Predictive study of tuberculosis incidence by time series method and elman neural network in kashgar, china. *BMJ Open*, 11(1), 1–8.